

# Josephson currents in neutron stars

Armen Sedrakian<sup>1,2</sup> and Peter B. Rau<sup>3</sup>

<sup>1</sup>Frankfurt Institute for Advanced Studies, D-60438 Frankfurt am Main, Germany

<sup>2</sup>Institute of Theoretical Physics, University of Wrocław, 50-204 Wrocław, Poland\*

<sup>3</sup>Institute for Nuclear Theory, University of Washington, Seattle, Washington, 98195-4550 USA<sup>†</sup>

(Dated: January 3, 2025)

We demonstrate that the interface between  $S$ -wave and  $P$ -wave paired superfluids in neutron stars induces a neutron supercurrent, a charge-neutral analog of the Josephson junction effect in electronic superconductors. The proton supercurrent entrainment by the neutron superfluid generates, in addition to the neutral supercurrent, a charged current across the interface. Beyond this stationary effect, the motion of the neutron vortex lines responding to secular changes in the neutron star's rotation rate induces a time-dependent oscillating Josephson current across this interface when proton flux tubes are dragged along with them. We show that such motion produces radiation from the interface once clusters of proton flux tubes intersect the interface. The power of radiation exceeds by orders of magnitude the Ohmic dissipation of currents in neutron stars. This effect appears to be phenomenologically significant enough to heat the star and alter its cooling rate during the photon cooling era.

PACS numbers: 21.65.+f, 21.30.Fe, 26.60.+c

## I. INTRODUCTION

Neutron stars are unique objects where quantum physics manifests itself on stellar-size macroscopic scales as their rotational dynamics and magnetic fields are supported by quantized vortex networks extending over macroscopic scales; for reviews, see Refs. [1, 2]. At low densities, their inner crust contains a neutron superfluid, which forms spin-zero Cooper pairs due to nuclear attraction in the  $^1S_0$  partial wave channel. At high densities, corresponding to the core of the star, the dominant attractive partial wave channel is the  $^3P_2$ - $^3F_2$ ; i.e., neutrons are paired in a spin-one state [3, 4]. An alternative  $P$ -wave channel at high density is the  $^3P_0$  channel if the  $^3P_2$ - $^3F_2$  pairing is suppressed by the spin-orbit interaction [5]. The density at which crust-core transition occurs is given by the density  $n^\ddagger \simeq 0.5n_0 = 0.08 \text{ fm}^{-3}$ , which is defined by the dissolution of protons bound in nuclei into a continuum, forming a fluid [6]. As seen from Fig. 1, the transition from  $S$ - to  $P$ -wave neutron superfluid occurs at about the same density. Unbound protons at and above  $0.5n_0$  pair in the spin-zero  $S$ -state and are admixed with the  $P$ -wave neutron superfluid. The transition between  $S$  and  $P$ -wave superfluids can occur either at a sharp interface or via a formation of a mixture of these phases within some density domain. We will assume a sharp interface between the two superfluids, but we will briefly comment on the implications of a mixed phase.

The focus of this work is on the interface between two

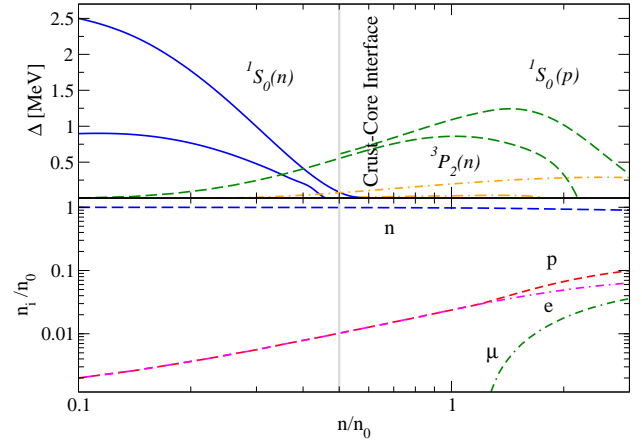


FIG. 1: Upper panel: dependence of pairing gaps for neutrons in  $^1S_0$  (solid lines) and  $^3P_2$ - $^3F_2$  (dot-dashed lines) and for protons in  $^1S_0$  (dashed lines) on baryonic density in units of nuclear saturation density. The upper and lower lines correspond to lower and upper bounds as discussed in Ref. [3]. Lower panel: composition of the core of a neutron star at  $T = 0$  used to obtain the gaps. The vertical line shows the crust-core interface at the density  $n/n_0 = 0.5$ .

neutral  $S$ -wave and  $P$ -wave superfluids. We show that a current emerges at this interface, in analogy to Josephson effects in metallic superconductors [7, 8], due to the difference in the phases of these superfluids. Specifically, we show the following stationary case:

- (a) a neutron superflow arises at the  $S$ -wave/ $P$ -wave superfluid interface due to the difference in the phases

\*Electronic address: [sedrakian@fias.uni-frankfurt.de](mailto:sedrakian@fias.uni-frankfurt.de)

<sup>†</sup>Present address: Columbia Astrophysics Laboratory, Columbia University, New York, New York 10027 USA; Electronic address: [peter.rau@columbia.edu](mailto:peter.rau@columbia.edu)

of these superfluids, i.e., the interface acts as a Josephson junction. An analogous effect in neutral superfluid ultracold atomic gases has been observed recently [9].

- (b) Because of the entrainment of the protons by the motion of the neutrons [10–12], the neutron superflow induces a charged current through the interface as well.
- (c) Going beyond the stationary limit, we show that a type of non-equilibrium Josephson effect arises because the star changes its spin frequency on secular timescales.

Neutron superfluid rotates by forming an array of quantum vortices and the proton superconductor is type II at relevant densities and sustains flux tubes that carry the magnetic flux of the star within the superconducting regions [1, 2, 13–15]. The secular deceleration of neutron stars due to (primarily) their magnetic dipole radiation leads to an expansion of the neutron vortex lattice and neutron vortex lines (and eventually proton flux tubes) crossing the interface. This time-dependent process leads to the current oscillations through the interface—an analog of the time-dependent Josephson effect. The dynamics of a coupled network of neutron vortex and proton flux tube arrays is not well understood over timescale characteristic for glitches and their relaxation due to their complexity. Below, we assume that the flux tubes comove (on secular time scales) with neutron vortices and show that the crust-core interface radiates electromagnetically. The amount of radiation emitted by the flux tubes is significant enough to deposit phenomenologically important amounts of heat at the crust-core interface, thereby altering the cooling behavior of neutron stars. We do not address the problem of glitches, which can be associated with the interfaces between various phases, in particular superfluids; see, for example, Refs. [16–18].

## II. STATIONARY CURRENTS ACROSS THE INTERFACE

Consider a setup where the interface is the  $yz$  plane of a Cartesian coordinate system. The  $x > 0$  region corresponds to  $S$ -wave neutron ( $n$ ) superfluid characterized by an equilibrium Ginzburg-Landau (GL) order parameter (wave function)  $\psi_{1,n}^\infty$  and the  $x < 0$  region corresponds to  $P$ -wave superfluids with GL wave function  $\psi_{2,n}^\infty$ . This is illustrated in Fig. 2. A  $P$ -wave superfluid has a more complex order parameter [19–25] than the scalar one adopted here, but the spin dynamics of the Cooper pairs is not essential for our discussion.

The equations of motion for the wave functions  $\psi_{p/n}$  of proton ( $p$ ) and neutron ( $n$ ) condensates (i.e. the first GL equations) are derived in Appendix A and are given

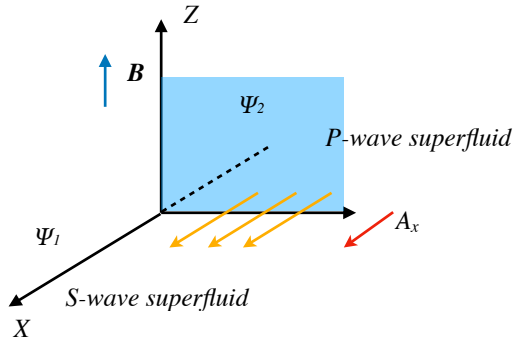


FIG. 2: Illustration of the local setup to compute the Josephson current. The interface, separating the superfluids, is the  $yz$  plane with  $x > 0$  corresponding to the  $S$ -wave condensate and  $x < 0$  to the  $P$ -wave condensate. The Josephson current (yellow arrows) flows across the interface parallel to the  $x$ -axis. In the case of proton flux tubes the magnetic field  $\mathbf{B}$  is locally along the  $z$ -axis and the vector potential  $\mathbf{A}$  varies along the  $x$ -axis, while its constant  $y$ -component does not contribute to its curl.

by

$$a_p \psi_p + b_p |\psi_p|^2 \psi_p + g_{np} |\psi_n|^2 \psi_p + \frac{1}{4m_p} \left( -i\hbar \nabla - \frac{2e}{c} \mathbf{A} \right)^2 \psi_p = 0, \quad (1)$$

$$a_n \psi_n + b_n |\psi_n|^2 \psi_n + g_{np} |\psi_p|^2 \psi_n - \frac{\hbar^2}{4m_n} \nabla^2 \psi_n = 0, \quad (2)$$

where  $a_{n,p} < 0$  in the superfluid state,  $b_{n,p} > 0$ ,  $\mathbf{A}$  is the vector potential,  $e > 0$  is the unit charge,  $g_{np}$  describes the coupling between the amplitudes of the condensates,  $c$  is the speed of light and  $m_{n/p}$  are the bare masses of the neutron/proton. The boundary condition at the interface between the superfluids is a generalization of the ordinary GL boundary conditions to account for the tunneling of the pairs across the boundary [8]

$$\mathbf{n} \cdot \left( \nabla - \frac{2ie}{\hbar c} \mathbf{A} \right) \psi_{1,2,j} \Big|_{\text{Boundary}} = \pm \frac{\psi_{2,1,j} \Big|_{\text{Boundary}}}{\zeta_j}, \quad (3)$$

where  $j = n, p$ , the coefficient  $\zeta_{n/p}^{-1}$  is proportional to the permeability of the barrier between the superfluids [7] and  $\mathbf{n}$  is the unit vector orthogonal to the boundary. The proton charge current density and neutron mass current density are obtained by variation of the GL functional with respect to the vector potential  $\mathbf{A}$  and neutron ve-

locity  $\mathbf{v}_n$ , respectively:

$$\begin{aligned} \mathbf{j}_p &= \frac{e\hbar}{2im_p} \left(1 - \frac{\rho_{pn}}{\rho_{pp}}\right) (\psi_p^* \nabla \psi_p - \psi_p \nabla \psi_p^*) \\ &\quad + \frac{e\hbar}{2im_p} \frac{\rho_{pn}}{\rho_{nn}} (\psi_n^* \nabla \psi_n - \psi_n \nabla \psi_n^*) \\ &\quad - \frac{e^2}{m_p^2 c} (\rho_{pp} - \rho_{pn}) \mathbf{A}, \end{aligned} \quad (4)$$

$$\begin{aligned} \mathbf{j}_n &= \frac{\hbar}{2i} \left(1 - \frac{\rho_{pn}}{\rho_{nn}}\right) (\psi_n^* \nabla \psi_n - \psi_n \nabla \psi_n^*) \\ &\quad + \frac{\hbar}{2i} \frac{\rho_{pn}}{\rho_{pp}} (\psi_p^* \nabla \psi_p - \psi_p \nabla \psi_p^*) - \frac{e}{m_p c} \rho_{pn} \mathbf{A}. \end{aligned} \quad (5)$$

The derivation of these equations and definition of the elements of the density matrix  $\rho_{ij}$ ,  $i, j \in p, n$  are given in Appendix A. The off-diagonal term  $\rho_{pn} = \rho_{np}$  describes the kinetic coupling between the two condensates known as *entrainment*. The combination of (3) with (4) and (5), and the requirement of invariance upon a gauge transformation  $\mathbf{A} \rightarrow \mathbf{A} + \nabla\alpha$  for a scalar function  $\alpha$  give the Josephson currents across the interface

$$\begin{aligned} \mathbf{n} \cdot \mathbf{j}_p &= \frac{e\hbar}{m_p \zeta_p} \frac{(\rho_{pp} - \rho_{pn})}{\rho_{pp}} |\psi_{1,p}| |\psi_{2,p}| \sin(\Delta\theta_p) \\ &\quad + \frac{e\hbar}{m_p \zeta_n} \frac{\rho_{pn}}{\rho_{nn}} |\psi_{1,n}| |\psi_{2,n}| \sin(\Delta\theta_n). \end{aligned} \quad (6)$$

$$\begin{aligned} \mathbf{n} \cdot \mathbf{j}_n &= \frac{\hbar}{\zeta_n} \frac{\rho_{nn} - \rho_{pn}}{\rho_{nn}} |\psi_{1,n}| |\psi_{2,n}| \sin(\Delta\theta_n) \\ &\quad + \frac{\hbar}{\zeta_p} \frac{\rho_{pn}}{\rho_{pp}} |\psi_{1,p}| |\psi_{2,p}| \sin(\Delta\theta_p), \end{aligned} \quad (7)$$

where we used  $\psi_j = |\psi_j| e^{i\theta_j}$  for  $j = n, p$  and where the gauge invariant phase difference is

$$\Delta\theta_i = \theta_{2,i} - \theta_{1,i} - \frac{2\pi}{\Phi_0} \delta_{i,p} \int_p \mathbf{A} \cdot d\mathbf{l}. \quad (8)$$

Here  $\Phi_0 = \pi\hbar c/e$  is the flux quantum for the proton ( $p$ ) condensate and  $\delta_{ip}$  is a Kronecker delta.

Equations (6) and (7) demonstrate that a stationary supercurrent flows across the interface between the  $S$ - and  $P$ -wave superfluids, driven by the phase difference  $\Delta\theta_n$  of the two superfluids. This phase difference arises from a change in the neutron pairing interaction, transitioning from  ${}^1S_0$  to  ${}^3P_2$ - ${}^3F_2$ -wave as the neutron density increases, as shown in Fig. 1. Additionally, Eq. (6) reveals that the entrainment effect results in a proton electric supercurrent across the interface, also induced by the phase difference  $\Delta\theta_n$ .

If uncoupled from the neutron condensate, the proton condensate order parameter is the same on both sides of the interface  $\psi_{1,p} = \psi_{2,p}$  and corresponds to  ${}^1S_0$  pairing, which is due to the lower density of protons compared to neutrons under  $\beta$ -equilibrium in neutron stars. However, because of the entrainment between the neutron

and proton condensate wave functions,  $\psi_{1,p}$  and  $\psi_{2,p}$  are no longer required to be equal if  $\psi_{1,n} \neq \psi_{2,n}$ . A density jump at the  $S$ - $P$  transition interface, either for neutrons or protons, is energetically implausible. Consequently, the magnitudes of their order parameters must remain continuous. Thus, the phase difference in the neutron condensate necessitates a corresponding phase difference in the proton condensate. This can be seen by examining the Ginzburg-Landau free energy, which should be equal on both sides of the junction since this is the condition for the transition from  $S$ - to  $P$ -wave neutron pairing. If the condensate densities are the same on both sides of the junction  $|\psi_{n,1}| = |\psi_{n,2}|$  and  $|\psi_{p,1}| = |\psi_{p,2}|$ , the only contribution to the Ginzburg-Landau free energy which can be different across the junction is the kinetic part, given by (see Appendix A)

$$\begin{aligned} F_{\text{kin}} &= \frac{\hbar^2}{8m_p^2} (\rho_{pp} - \rho_{pn}) \left( \nabla\theta_p - \frac{2e}{\hbar c} \mathbf{A} \right)^2 \\ &\quad + \frac{\hbar^2}{8m_n^2} (\rho_{nn} - \rho_{pn}) (\nabla\theta_n)^2 \\ &\quad + \frac{\hbar^2 \rho_{pn}}{4m_p m_n} \left( \nabla\theta_p - \frac{2e}{\hbar c} \mathbf{A} \right) \cdot \nabla\theta_n. \end{aligned} \quad (9)$$

We can evaluate  $F_{\text{kin}}$  on either side of the junction and set both sides equal to each other. For this equality to be true while the neutron phase is different across the junction  $\theta_{1,n} \neq \theta_{2,n}$ , either (a) the gradients in the neutron phases must be equal  $|\nabla\theta_{1,n}| = |\nabla\theta_{2,n}|$  or (b) the proton phase (or more specifically its gradient) must also be different across the junction. This leaves the possibility of  $\theta_{1,p} \neq \theta_{2,p}$ .

### III. TIME-DEPENDENT CURRENTS ACROSS THE INTERFACE

Neutron stars decelerate under the action of external braking torques, which leads to a decrease in the average number of quantum neutron vortices in the superfluid. By continuity, the number of neutrons vortices is reduced through their motion away from the rotation axis. Because of the entrainment, neutron vortices carry a fractional flux localized close to their cores. In addition, the stellar magnetic field in the type II superconducting core exists in the form of proton flux tubes, which will be rearranged by such motion. The average number of proton flux tubes intersecting the area occupied by a single neutron vortex is very large, of the order of  $n_\Phi/n_V \sim 10^{13}$ , where the number densities of proton flux tubes and neutron vortices are given by  $n_\Phi = \bar{B}/\Phi_0$ , and  $n_V = 2\Omega/\kappa$  with quantum circulation  $\kappa = \pi\hbar/m_n^*$  with  $m_n^*$  being the neutron (effective) mass. Here  $\Omega$  is the rotation frequency and  $\bar{B}$  is the average magnetic field. The field may be inhomogeneously distributed across a single neutron vortex. For, example, the vortex-cluster model envisions the clustering of proton flux tubes around the

neutron vortex [26]. The interaction between neutron vortex arrays and flux tubes in a type II superconductor is generally complex. This complexity arises from the unknown geometry of the flux tube arrays, which is dictated by the global magnetic field configuration of the star (e.g., poloidal versus toroidal), as well as the uncertain strength of the interactions between vortices and flux tubes. As limiting cases, one can envision two scenarios: in response to the star's deceleration and the motion of neutron vortices, the flux tubes could either move together with the vortices or remain anchored to the crustal magnetic field, staying motionless. Since our focus is on the long-term dynamics of the vortex-flux tube conglomerate over secular timescales, which are much longer than the typical timescales associated with glitches and post-glitch relaxations, we will assume that the flux tubes, when averaged over long timescales, move at the same speed as the neutron vortex array.

The motion of neutron vortex lines and proton flux tubes outward from the core of a neutron star will serve as a source of time-dependent Josephson currents across the  $S$ - $P$  neutron superfluid phase transition interface. Such a current requires a time-varying phase difference across the junction. A neutron vortex line passing through the junction will induce a time-dependent phase difference in the neutron superfluid. This is because in the core of a neutron vortex, the superfluidity is suppressed and outside this core, the phase of the order parameter depends on the distance from the axis of the vortex  $\varrho$  according to  $\nabla\theta_n = (1/\varrho)\hat{\varphi}$  (see Eqs. (A4) and (A5)) and thus changes logarithmically as  $\theta_n(\varrho) = \ln \varrho$  with the distance between the vortex and the interface, where  $\varrho$  and  $\varphi$  are the cylindrical radius and angle in the plane orthogonal to the vortex circulation.

If a neutron vortex is moving through the interface then the neutron order parameter will acquire a time-dependent phase

$$\Delta\theta_n = \theta_{1,n} - \theta_{2,n} + \omega_V t, \quad (10)$$

where  $\theta_{1,n}$  and  $\theta_{2,n}$  are the static phases on either side of the junction and  $\omega_V t$  is a time-dependent part induced by the motion of a neutron vortex line through the junction with period  $2\pi/\omega_V$ , with  $\omega_V = v_{Lr}/d_n$ , where  $v_{Lr}$  is the radial velocity of neutron vortex lines averaged over secular time scales and is given by

$$v_{Lr} = -\frac{\dot{\Omega}}{2\Omega}r, \quad (11)$$

where  $r$  is the cylindrical radius and  $d_n$  is the intervortex spacing. Equation (11) follows from the conservation of vortex number density  $n_V$ . Because of superfluid entrainment, the time-dependent neutron phase induces a time-dependent proton current through the junction given by

$$\mathbf{j}_V \equiv \mathbf{n} \cdot \mathbf{j}_p(t) = j_{0,pn} \sin(\theta_{2,n} - \theta_{1,n} + \omega_V t), \quad (12)$$

where

$$j_{0,pn} \equiv \frac{e\hbar}{m_p \zeta_n} \frac{\rho_{pn}}{\rho_{pp}} |\psi_{1,n}| |\psi_{2,n}|. \quad (13)$$

As we showed in the previous section, a time-dependent neutron phase difference can induce a time-dependent proton phase difference across the interface. Additionally, the motion of proton flux tubes through the junction will induce a time-dependent vector potential within the interface, so that the resulting gauge-invariant phase difference will be time dependent. Consider now a single flux tube crossing the interface between the two superfluids, moving along with the vortex lines. The tube is assumed to be locally straight and along the  $z$  axis of our setup and the current is flowing along the  $x$  axis. The variations of the vector potential are along the  $x$  axis so that the nonvanishing component is  $A_x(x) = -H_z(x)y$  (see Fig. 2). For this setup Eq. (8) for the protons can be written

$$\Delta\theta_p = \theta_{2,p} - \theta_{1,p} - \frac{4\pi y H_{0z} \lambda}{\Phi_0}, \quad (14)$$

where  $\lambda$  is the magnetic field penetration depth. To evaluate the integral in Eq. (8), we integrate between two points deep in the  $S$ - and  $P$ -wave superfluids, respectively, and use that the magnetic field of a flux tube is given as  $H_z(x) = H_{0z} \exp(-x/\lambda)$ , where we used the large-distance asymptotic form of the modified Bessel function  $K_0$ . The passage of a flux tube through the interface induces a time-dependent flux inside the junction. For a proton flux tube, this has a frequency  $\omega_p = v_{Lr}/d_p$ , where  $v_{Lr}$  is given by Eq. (11) since the neutron vortex lines transport the proton flux tube, and  $d_p$  is the interflux tube spacing. The maximal value of the flux  $\Phi_{\max}$  will correspond to the case where the flux tube coincides with the interface, which has a width of roughly  $2\xi_n$ , where  $\xi_n$  is of the order of the coherence length of the neutron superfluid. Therefore, the time-dependent flux can be written as

$$\Phi_*(t) = \Phi_{\max} \cos(\omega_p t), \quad \Phi_{\max} = 8\pi\xi H_{0z} \lambda. \quad (15)$$

Thus, the time-dependent part of the Josephson current (6) now arises from the proton phase difference and is given by

$$\mathbf{j}_\Phi = \mathbf{n} \cdot \mathbf{j}_p(t) = j_{0,pp} \sin[\theta_{2,p} - \theta_{1,p} + \phi(t)], \quad (16)$$

where

$$j_{0,pp} \equiv \frac{e\hbar}{m_p \zeta_p} \frac{(\rho_{pp} - \rho_{pn})}{\rho_{pp}} |\psi_{1,p}| |\psi_{2,p}|, \quad \phi(t) = \frac{\Phi_*(t)}{\Phi_0} \quad (17)$$

The passage of a flux tube array through the interface thus induces an oscillating Josephson current in the interface. Due to the entrainment effect, the neutron vortex lines are also magnetized, and so a neutron vortex passing through the junction will also induce a time-dependent phase difference in the proton condensate. However, the

quantized flux within a neutron vortex is reduced compared to its value in a proton flux tube, and since the number density of proton flux tubes is much greater than of neutron vortex lines  $n_\Phi \gg n_V$ , we neglect the magnetization of the latter here.

#### IV. RADIATION FROM THE INTERFACE OF TWO SUPERFLUIDS

A time-oscillating Josephson current will lead to radiation of energy from the interface. The time-average power radiated by an oscillating current is given by

$$\langle P \rangle = \frac{2\langle \dot{I}^2 \rangle d^2}{3c^3}, \quad (18)$$

where  $\langle \dots \rangle$  denotes a time average,  $I$  is the current, and  $d$  is the length scale over which the current oscillates.

To obtain the power radiated over the entire star requires specifying the geometry of the problem. We assume that the spin axis is along the  $z$  direction of the cylindrical or polar direction of the spherical coordinate system, the former dictated by the geometry of the neutron vortex lattice and the latter by the spherical shape of the star, see Fig. 3. For the sake of simplicity, we assume that the interface between the superfluids is a cylinder coaxial with the rotation axis, with a height  $\ell_z \leq R$  centered at the equator. We will associate each neutron vortex with a cluster of proton flux tubes, as indicated in the previous section. We note that in spherical geometry only a segment of a flux, at any given time, crosses the interface; therefore, the approximation  $\ell_z \leq R$  might appear unjustified. However, consider moving from the North Pole of the star toward the equator along a meridian. As one proceeds, the path will intersect with vortices and associated flux tubes, which are spaced at microscopic distances from each other. Therefore, the entire meridian will contribute to radiation, even though at any given point, a different flux tube will be radiating.

We begin by estimating the radiation from a single neutron vortex lines passing through a junction. To obtain the power radiated per vortex crossing the interface we use the expression  $I = j(\ell_\perp \ell_z)$ , where  $j = j_V$  from Eq. (12) is the Josephson current and  $\ell_\perp$  and  $\ell_z$  are the extent of the junction perpendicular to/along the  $z$  direction respectively. We find

$$\langle P_V \rangle = \frac{(j_{0,pn}\omega_V)^2}{3c^3} (d\ell_\perp \ell_z)^2. \quad (19)$$

The radiant power from this mechanism for the entire star,  $\mathcal{P}_{*,V}$ , can be estimated by approximating the spherical geometry of the interface with an “effective” cylinder of radius  $R$  and height  $\ell_z \sim R$ , as explained above. The number of vortices on this cylinder at any time is determined by the ratio of its circumference to the neutron intervortex distance, i.e.,  $N_V = 2\pi R/d_n$ . Multiplying Eq. (19) by the number of vortex lines  $N_V$ , one finds

$$\langle \mathcal{P}_{*,V} \rangle = 3 \times 10^7 \tau_5^{-2} R_6^5 \Omega_{100}^{3/2} \text{ erg s}^{-1}, \quad (20)$$

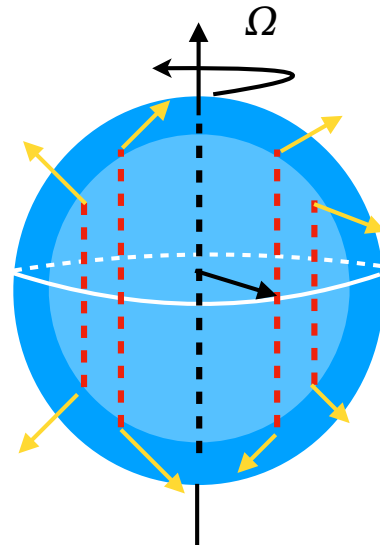


FIG. 3: Illustration of the computation of radiation (yellow arrows) at the interface between  $S$ - and  $P$ -wave superfluids. A collection of vortices or flux tubes (red lines) cross the interface. The effective macroscopic length over which radiation is taking place is of the order of  $R$ .

where  $\tau_5$  is the spin-down lifetime in units of  $10^5$  yr,  $R_6$  is the stellar radius in units of  $10^6$  cm, and  $\Omega_{100}$  is the rotation angular frequency in units of  $100 \text{ s}^{-1}$ . We approximated  $d \sim \ell_\perp \sim \lambda$  and  $\ell_z \sim R$ . The details of the computation are given in Appendix B.

The value in Eq. (20) is far too low to be observationally interesting. For instance, it is far smaller than the heating power due to the Ohmic dissipation of the crustal magnetic field  $B_{\text{cr}}$  on a typical scale  $\delta R$

$$\mathcal{P}_O \simeq 10^{27} \left( \frac{B_{\text{cr}}}{10^{13} \text{ G}} \right)^2 \left( \frac{10^{23} \text{ s}^{-1}}{\sigma} \right) \left( \frac{\delta R}{0.5 \text{ km}} \right) \text{ erg s}^{-1}, \quad (21)$$

where  $\sigma$  is crustal electric conductivity.

We now consider the radiation from a single proton flux tube passing through a junction. Using  $I = j_\Phi(\ell_\perp \ell_z)$  in Eq. (18), with  $j_\Phi$  given by Eq. (16), leads to

$$\begin{aligned} \langle P_\Phi \rangle &= \frac{2(j_0\omega_p)^2}{3c^3} (d\ell_\perp \ell_z)^2 \langle \cos^2(\Delta\theta_p + \phi(t)) \sin^2(\omega_p t) \rangle, \\ &= \frac{(j_0\omega_p)^2}{6c^3} (d\ell_\perp \ell_z)^2, \end{aligned} \quad (22)$$

where we approximated the time average

$$\begin{aligned} &\langle \cos^2(\Delta\theta_p + \phi(t)) \sin^2(\omega_p t) \rangle \\ &= \frac{1}{4} \{1 + J_1(2) \cos(2\Delta\theta_p)\} \simeq \frac{1}{4}, \end{aligned} \quad (23)$$

where  $J_1(x)$  is a Bessel function and where we average over the possible phase differences  $\Delta\theta_p$ .

According to our conjecture, the flux tubes are transported by neutron vortex array over secular timescales with the average velocity equal to the vortex line velocity Eq. (11). The oscillation frequency of the time-dependent current  $\omega_p$  is thus an average and depends on the actual arrangement of the flux tubes in any particular model. Therefore, the estimate of radiation power below should be viewed as an estimate of the average output only. The details of the computation of the power of radiation are given in Appendix B. The final result is

$$\langle P_{*,\Phi} \rangle = 2 \times 10^{28} \tau_5^{-2} R_6^5 B_{13}^{3/2} \text{ erg s}^{-1}, \quad (24)$$

where  $B_{13}$  is the magnetic field in units  $10^{13}$  G.

The value quoted in Eq. (24) can be compared to Eq. (21). Unlike the heating caused by Josephson radiation linked to the time-dependent neutron phase from neutron vortex lines intersecting the  $S$ - $P$  interface, the heating due to the time-dependent proton phase from proton flux tubes crossing the  $S$ - $P$  interface is approximately an order of magnitude greater than the Ohmic dissipation (21), which is typically regarded as a primary heating mechanism in neutron stars.

## V. CONCLUSIONS

In this work, we argued that the interface between  $S$ -wave and  $P$ -wave superfluids can function like a Josephson junction, where a supercurrent arises from the phase differences between the two superfluids. We have shown that there is a stationary neutron current across the interface due to this phase difference, which also entrains part of the proton condensate thus generating a stationary flow of protons across the interface. Beyond this stationary effect, the movement of neutron vortices and proton flux tubes generates time-dependent Josephson currents, oscillating at a frequency determined by the interflux tube spacing and neutron vortex velocity.

A time-dependent electromagnetic current generates radiation. With this in mind, we have demonstrated that the Josephson junction between  $S$ - and  $P$ -superfluids produces electromagnetic radiation at the interface, heating the star. Specifically, the amount of heat generated by the time-dependent Josephson current induced by proton flux tubes entering the junction is phenomenologically significant and can impact the late-time cooling of neutron stars. The heating rate is independent of temperature but depends on the spin frequency and its derivative, as well as the strength of the magnetic field. Here, we assumed a sharp interface between the  $S$ -wave and  $P$ -wave superfluids. However, if the transition between these phases occurs through a mixed phase, the

radiation will be amplified due to the “stacking” of multiple Josephson-like junctions along the path of a flux tube cluster carried by a neutron vortex. To confirm the astrophysical importance of radiation from oscillating Josephson currents, cooling simulations of neutron stars that incorporate the discussed heating mechanism would be necessary. Such thermal cooling simulations must also integrate the neutron star’s secular deceleration dynamics under braking torques, such as magnetic dipole radiation while accounting for the long-term evolution of the magnetic field.

We emphasize that the mechanism discussed here operates effectively on secular timescales and is not currently suitable for modeling transient phenomena in pulsar rotation, such as glitches. Moreover, its validity hinges on the assumption that, on average, flux tubes move together with neutron vortices. This assumption breaks down if neutron vortices are able to cut through flux tubes, leaving the latter stationary—a scenario that arises when significant restoring forces act on the flux tubes at their edges on the crust-core boundary.

The dissipative process under consideration arises from the motion of neutron vortices, which reduces their number in the core. As a result, the rotational energy of the neutron superfluid serves as the ultimate energy source, with the associated radiation effectively acting as frictional dissipation at the boundary. This dissipation contributes to the internal torque transmitted from the superfluid core to the crust, which is incorporated into the coupled equations of motion for the two-fluid model with internal friction [see, for example, Ref. [27], Eqs. (4) and (5)].

Finally, entrainment-induced nonstationary Josephson currents and radiation proposed here may have analogs in other systems, for example, in ultracold atomic systems, where Josephson junctions have been recently manufactured [9]. Entrainment would require mixtures of atoms, whereas the electric current and radiation would require a charged component or artificial gauge fields [28]. Such a setup is expected to work with any combination of Fermi or Bose condensates, whether interfacing with each other or forming mixtures.

## Acknowledgments

We thank Ira Wasserman for useful discussions. A.S. acknowledges support through Deutsche Forschungsgemeinschaft Grant No. SE 1836/5-3, and the Polish NCN Grant No. 2020/37/B/ST9/01937. P.B.R. was supported by the Institute for Nuclear Theory’s U.S. Department of Energy Grant No. DE-FG02-00ER41132.

## Appendix A: Ginzburg-Landau model of superfluid neutron and superconducting proton fluids

The Ginzburg-Landau theory provides a phenomenological framework to describe fermionic superconductors and superfluids near their critical points. Here, we describe a GL model for a proton superconductor and a neutron superfluid, which extends the original GL theory to account for coupling between the fluids. In the context of neutron stars such models were developed by various authors [10, 11, 29, 30].

Consider a proton superconductor with an order parameter  $\psi_p$  and the neutron superfluid with an order parameter  $\psi_n$ . The general GL free energy functional can be written as

$$F = F_0 + F_{\text{kin}} + F_{\text{cond}} + F_{\text{em}}, \quad (\text{A1})$$

where  $F_0$  is the bulk free energy in the normal state,  $F_{\text{kin}}$  is the kinetic energy contribution which involves the gradients of the order parameter,  $F_{\text{cond}}$  is the condensate term involving the order parameters, and  $F_{\text{em}}$  is the electromagnetic field contribution. The energy is typically measured from  $F_0$ ; therefore, it can be dropped below. The condensation part is given by

$$F_{\text{cond}} = a_p |\psi_p|^2 + \frac{b_p}{2} |\psi_p|^4 + a_n |\psi_n|^2 + \frac{b_n}{2} |\psi_n|^4 + g_{np} |\psi_p|^2 |\psi_n|^2, \quad (\text{A2})$$

where the coefficients  $a_{p/n}$  and  $b_{p/n}$  have their usual meaning in the GL theory for superfluidity/superconductivity [31], and the term  $\propto g_{np}$  describes the coupling between the two condensates. The part of the free-energy functional which represents the kinetic energy contributions of two coupled fluids, with velocities  $\mathbf{v}_p$  and  $\mathbf{v}_n$  is given by

$$F_{\text{kin}} = \frac{1}{2} \rho_{pp} v_p^2 + \frac{1}{2} \rho_{nn} v_n^2 - \frac{1}{2} \rho_{pn} |\vec{v}_p - \vec{v}_n|^2, \quad (\text{A3})$$

where  $\mathbf{v}_p$  and  $\mathbf{v}_n$  refer to the velocities of the fluids and  $\rho_{pp}$  and  $\rho_{nn}$  are the effective densities for the superconductor and superfluid, respectively.  $\rho_{pn}$  represents the coupling between the two systems. These densities have been derived using specific nuclear models [32, 33] and can be expressed in terms of the effective masses of neutrons, protons, and their partial densities  $\rho_n$  and  $\rho_p$ .

In the GL theory for superconductors and superfluids, the velocities  $\mathbf{v}_p$  and  $\mathbf{v}_n$  can be associated with the phase gradients of the complex order parameters  $\psi_p$  and  $\psi_n$ . Writing the wave function with the magnitude and the phase  $\psi_j = |\psi_j| e^{i\theta_j}$  for  $j = n, p$ , the velocities are given by the phase gradient of the order parameter, plus the coupling to the vector potential for the protons,

$$\mathbf{v}_n = \frac{\hbar}{2m_n} \nabla \theta_n, \quad \mathbf{v}_p = \frac{\hbar}{2m_p} \left( \nabla \theta_p - \frac{2e}{\hbar c} \mathbf{A} \right), \quad (\text{A4})$$

where  $\hbar$  is the Planck constant,  $m_n/m_p$  is the mass of the neutron/proton, and  $\theta_n/\theta_p$  is the phase of the superfluid neutron/superconducting proton order parameter. A factor  $2e$  appears instead of  $e$  for the coupling of the protons to  $\mathbf{A}$  because the superconducting protons form Cooper pairs with charge  $2e$ . Substituting Eqs. (A4) into Eq. (A3), we obtain Eq. (9) of the main text.

The velocity field of a quantized neutron vortex using the cylindrical coordinates  $(\varrho, \varphi, z)$  is given by

$$\mathbf{v}_n = \frac{n\hbar}{2m_n\varrho} \hat{\varphi} \quad (\text{A5})$$

where  $n$  is the quantum number (in the ground state of lowest energy  $n = 1$ )  $\varrho$  is the distance from the vortex center,  $\hat{\varphi}$  is the angle variable with  $z$  axis along the neutron vortex. For the proton flux tube, the velocity field is given by

$$\mathbf{v}_p = \frac{\Phi_0}{2\pi\lambda} K_1 \left( \frac{\varrho}{\lambda} \right) \hat{\varphi}, \quad (\text{A6})$$

where  $K_1(\varrho/\lambda)$  is the modified Bessel function of the second kind, which describes the radial decay of the velocity around the flux tube.

Finally, the electromagnetic field contribution to  $F$  is

$$F_{\text{em}} = \frac{(\nabla \times \mathbf{A})^2}{8\pi}. \quad (\text{A7})$$

We assume that there is also an overall electrically neutralizing lepton fluid such that there are no electric fields in the problem.

The dynamics of ordinary GL theory is described by two equations of motion that follow from the variation of the GL functional with respect to the order parameter and electromagnetic field potential  $\mathbf{A}$ , respectively. The number of equations of motion doubles in the present case. The equations of motion for the proton and neutron order parameters  $\psi_p$  and  $\psi_n$  are found by minimizing the free energy with respect to  $\psi_n^*/\psi_p^*$  respectively, which leads to Eqs. (1) and (2). These are the coupled GL equations for the proton superconductor and neutron superfluid, accounting for their interactions as well as the coupling of the proton superconductor to the electromagnetic field.

To obtain the second set of GL equations, which provides the proton charge current density and the neutron mass current density, we vary  $F$  with respect to  $\mathbf{A}$  and  $\mathbf{v}_n$  respectively, giving

$$\mathbf{j}_p = \frac{e\hbar}{2m_p^2} (\rho_{pp} - \rho_{pn}) \left( \nabla\theta_p - \frac{2e}{\hbar c} \mathbf{A} \right) + \frac{e\hbar}{2m_p m_n} \rho_{pn} \nabla\theta_n, \quad (\text{A8})$$

$$\mathbf{j}_n = \frac{\hbar}{2m_n} (\rho_{nn} - \rho_{pn}) \nabla\theta_n + \frac{\hbar}{2m_p} \rho_{pn} \left( \nabla\theta_p - \frac{2e}{\hbar c} \mathbf{A} \right). \quad (\text{A9})$$

Unlike the ordinary currents in the GL theory, these expressions depend on the phase gradients of both order parameters, coupled through the entrainment parameter  $\rho_{np}$ .

For the discussion of the junction, it is useful to eliminate the phase gradients  $\nabla\theta_{p/n}$  from the expressions for the currents. This is done using the relation

$$(\psi_j^* \nabla\psi_j - \psi_j \nabla\psi_j^*) = 2i |\psi_j|^2 \nabla\theta_j = i \frac{\rho_{jj}}{m_j} \nabla\theta_j, \quad (\text{A10})$$

where we substituted  $\psi_j = |\psi_j| e^{i\theta_j}$ ,  $j = n, p$  and defined  $2m_j |\psi_j|^2 = \rho_{jj}$ . Using this relation, Eqs. (A8) and (A9) can be written in the forms Eqs. (4) and (5), respectively.

## Appendix B: Computing the power of radiation

We first show the computation of Eq. (20). Substituting the velocity of the vortex lattice in the radiation formula we obtain (19)

$$\langle P_V \rangle = \frac{(j_{0,pn} \omega_V)^2}{3c^3} (d\ell_\perp \ell_z)^2 = \frac{j_{0,pn}^2}{3c^3} \left( \frac{d\ell_\perp \ell_z}{d_n} \right)^2 \left( \frac{\dot{\Omega}}{2\Omega} \right)^2 r^2. \quad (\text{B1})$$

To evaluate  $j_{0,pn}$ , we assume  $|\psi_{1,n}| \approx |\psi_{2,n}|$ , because a density jump at the  $S$ - $P$  interface is not expected. We also set  $\rho_j = m_j n_j = 2m_j^* |\psi_j|^2$ ,  $j = n, p$ , to define the bare mass density in terms of the effective mass  $m_j^*$  and  $|\psi_j|^2$ . We thus find

$$j_{0,pn} = \frac{e\hbar}{m_p \zeta_n} \frac{\rho_{pn}}{\rho_{pp}} |\psi_n|^2 = e \eta_n v_{Fn} n_n, \quad \kappa_{np} \equiv \frac{\rho_{pn}}{\rho_{pp}}, \quad \eta_n \equiv \frac{\kappa_{np}}{2\zeta_n k_{Fn}}, \quad (\text{B2})$$

where we introduced the neutron Fermi wave-vector  $k_{Fn}$  and velocity  $v_{Fn} = \hbar k_{Fn} / m_n^*$ .

The problem involves two distinct characteristic scales: 1) a microscale, on the order of 100 fm, which corresponds to the penetration depth,  $\lambda$ , or several times the coherence length, which represents the width of the Josephson junction, and 2) a macroscale, on the order of the interface radius,  $R$ . We then approximate

$$d \simeq l_\perp \simeq \lambda, \quad l_z \simeq R. \quad (\text{B3})$$

To find the radiation from the entire interface (on the stellar scale), we replace the spherical surface of the interface of two superfluids with an “effective cylinder” and multiply the radiation formula (B1) by the number of vortex lines on this cylinder  $2\pi R/d_n$ , i.e., this number is given by the circumference of the cylinder divided by the intervortex line distance. Thus, substituting also the expression for the supercurrent amplitude (B2) we obtain

$$\begin{aligned} \langle P_{*,V} \rangle &= \frac{2\alpha_e \pi \hbar}{3c^2} \left( \frac{R}{d_n} \right) (\eta_n v_{Fn} n_n)^2 \left( \frac{d\ell_\perp \ell_z}{d_n} \right)^2 \left( \frac{\dot{\Omega}}{2\Omega} \right)^2 r^2 \\ &= \frac{\alpha_e \pi \eta_n^2}{6} \left( \frac{v_{Fn}}{c} \right)^2 (n_n \lambda^2 R)^2 \left( \frac{R}{d_n} \right)^3 \frac{\hbar}{\tau^2}, \end{aligned} \quad (\text{B4})$$

where  $\alpha_e = e^2/\hbar c \approx 1/137$  and in the second step we introduced the pulsar lifetime  $\tau^{-1} = |\dot{\Omega}|/\Omega$  and set the location of the interface at  $r = R$ . To obtain the numerical estimate of the power of radiation we identify the location of the transition density from  $S$ -wave to  $P$ -wave superfluidity at the density of the crust-core interface  $n^\sharp = 0.08 \text{ fm}^{-3}$ . The radius of the cylindrical interface is thus  $R \approx 10^6 \text{ cm}$ .

Next is the computation of Eq. (24). Analogous manipulations to those for the neutron vortex line-induced Josephson current case result in

$$\langle P_{*,\Phi} \rangle = \frac{\alpha_e \pi \eta_p^2}{12} \left( \frac{v_{Fp}}{c} \right)^2 (n_p \lambda^2 R)^2 \left( \frac{R}{d_p} \right)^3 \frac{\hbar}{\tau^2}, \quad (\text{B5})$$

where we have defined a proton Fermi velocity  $v_{Fp}$  analogously to  $v_{Fn}$ , and where

$$\eta_p \equiv \frac{1 - \kappa_{np}}{2\zeta_p k_{Fp}}. \quad (\text{B6})$$

To make further progress, we need to estimate the order of magnitude of the microparameters of the proton and neutron condensate. For fixed  $n^\sharp = 0.08 \text{ fm}^{-3}$ , the effective mass values are  $m_p^*/m_p \approx 0.8$  and  $m_n^*/m_n \approx 0.9$ , as calculated at this density in Ref. [33]. The neutron Cooper pairing gap at this density is approximated by  $\Delta_n = 0.1 \text{ MeV}$  although variations can occur depending on the many-body approximations involved [3]. The neutron Fermi wave number, Fermi velocity, and coherence length are thus

$$k_{Fn} = (3\pi^2 n_n)^{1/3} = 1.33 \text{ fm}^{-1}, \quad \frac{v_{Fn}}{c} = \frac{\hbar k_{Fn}}{m_n^* c} = 0.28 \left( \frac{m_n}{m_n^*} \right) = 0.31 \left( \frac{0.9}{m_n^*/m_n} \right), \quad (\text{B7})$$

$$\xi_n(n_n^\sharp) = \frac{\hbar^2 c^2 k_{Fn}}{\pi m_n^* c^2 \Delta_n} = 195 \left( \frac{k_{Fn}}{1.33 \text{ fm}^{-1}} \right) \left( \frac{0.9}{m_n^*/m_n} \right) \left( \frac{0.1 \text{ MeV}}{\Delta_n} \right) \text{ fm}. \quad (\text{B8})$$

The neutron intervortex distance is

$$d_n = \left( \frac{\pi \hbar}{\sqrt{3} m_n^* \Omega} \right)^{1/2} = 3.56 \times 10^{-3} \left( \frac{0.9}{m_n^*/m_n} \right)^{1/2} \left( \frac{100 \text{ s}^{-1}}{\Omega} \right)^{1/2} \text{ cm}. \quad (\text{B9})$$

Finally, the parameter  $\eta_n$  is computed, using  $\kappa_{np} = m_p^*/m_p - 1 = -0.15$  [32] and  $\zeta_n \approx 2\xi_n$ ,

$$\eta_n = \frac{\kappa_{pn}}{2\zeta_n k_{Fn}} = -1.4 \times 10^{-4} \left( \frac{\kappa_{pn}}{-0.15} \right) \left( \frac{195 \text{ fm}}{\xi_n} \right) \left( \frac{1.33 \text{ fm}^{-1}}{k_{Fn}} \right). \quad (\text{B10})$$

For the protons, we assume a proton fraction 1% of total nucleonic density at the interface (see Fig. 1). We then find the proton Fermi wave number and Fermi velocity

$$k_{Fp} = (3\pi^2 n_p)^{1/3} = 0.29 \left( \frac{x_p}{0.01} \right)^{1/3} \text{ fm}^{-1}, \quad \frac{v_{Fp}}{c} = \frac{\hbar k_{Fp}}{m_p^* c} = 0.061 \left( \frac{m_p}{m_p^*} \right) = 0.076 \left( \frac{0.8}{m_p^*/m_p} \right). \quad (\text{B11})$$

The proton coherence length and magnetic field penetration depth are given by, using a proton Cooper pairing gap of  $\Delta_p = 0.1 \text{ MeV}$ ,

$$\xi_p(n_p^\sharp) = \frac{\hbar^2 c^2 k_{Fp}}{\pi m_p^* c^2 \Delta_p} = 48 \left( \frac{k_{Fp}}{0.29 \text{ fm}^{-1}} \right) \left( \frac{0.8}{m_p^*/m_p} \right) \left( \frac{0.1 \text{ MeV}}{\Delta_p} \right) \text{ fm}, \quad (\text{B12})$$

$$\lambda(n_p^\sharp) = \left( \frac{m_p^* c^2}{4\pi n_p \hbar c \alpha_e} \right)^{1/2} = 228 \left( \frac{m_p^*/m_p}{0.8} \right)^{1/2} \left( \frac{0.01}{x_p} \right)^{1/2} \text{ fm}. \quad (\text{B13})$$

Using these parameters and  $1 - \kappa_{np} = 1.15$ , which follows from the value of  $m_p^*/m_p = 0.8$ , and taking  $\zeta_p \approx 2\xi_p$ , we find

$$\eta_p = \frac{1 - \kappa_{pn}}{2\zeta_p k_{Fp}} = 0.02 \left( \frac{1 - \kappa_{pn}}{1.15} \right) \left( \frac{48 \text{ fm}}{\xi_p} \right) \left( \frac{0.29 \text{ fm}^{-1}}{k_{Fp}} \right). \quad (\text{B14})$$

We also need the interflux tube distance  $d_p$ , which is obtained from flux density  $n_\Phi$

$$n_\Phi = \frac{B}{\Phi_0} = 4.8 \times 10^{19} \left( \frac{B}{10^{13} \text{G}} \right), \quad d_p = \left( \frac{2}{\sqrt{3}n_\Phi} \right)^{1/2} = 1.55 \times 10^{-10} \text{ cm}, \quad (\text{B15})$$

where  $B$  is the magnetic field induction. Substituting into Eqs. (B4) and (B5), the parameters evaluated above, we find Eqs. (20) and (24) of the main text. The values of various dimensionless ratios entering these expressions for the radiation are

$$\frac{\alpha_e \pi \eta_n^2}{6} = 7.49 \times 10^{-11}, \quad \left( \frac{v_{Fn}}{c} \right)^2 = 0.096, \quad (n_n \lambda^2 R)^2 = 1.73 \times 10^{45}, \quad \left( \frac{R}{d_n} \right)^3 = 2.22 \times 10^{25}, \quad (\text{B16})$$

$$\frac{\alpha_e \pi \eta_p^2}{12} = 7.64 \times 10^{-7}, \quad \left( \frac{v_{Fp}}{c} \right)^2 = 0.0058, \quad (n_p \lambda^2 R)^2 = 1.72 \times 10^{41}, \quad \left( \frac{R}{d_p} \right)^3 = 2.68 \times 10^{47}, \quad (\text{B17})$$

and finally,  $\hbar/\tau_5^2 = 10^{-52} \text{ erg s}^{-1}$ .

- 
- [1] V. Graber, N. Andersson and M. Hogg, *Neutron stars in the laboratory*, *International Journal of Modern Physics D* **26** (2017) 1730015–347, [1610.06882].
- [2] B. Haskell and A. Sedrakian, *Superfluidity and Superconductivity in Neutron Stars*, *Astrophys. Space Sci. Libr.* **457** (2018) 401–454, [1709.10340].
- [3] A. Sedrakian and J. W. Clark, *Superfluidity in nuclear systems and neutron stars*, *European Physical Journal A* **55** (2019) 167, [1802.00017].
- [4] N. Chamel, *Superfluidity and Superconductivity in Neutron Stars*, *Universe* **10** (2024) 104.
- [5] E. Krotscheck, P. Papakonstantinou and J. Wang, *Triplet Pairing in Neutron Matter*, *Astrophys. J.* **955** (2023) 76, [2305.07096].
- [6] G. Grams, R. Somasundaram, J. Margueron and S. Reddy, *Properties of the neutron star crust: Quantifying and correlating uncertainties with improved nuclear physics*, *Phys. Rev. C* **105** (2022) 035806, [2110.00441].
- [7] L. D. Landau, E. M. Lifshitz and L. P. Pitaevskii, *Statistical Mechanics Part 2: Theory of the Condensed State*. Pergamon Press, Oxford, 1980.
- [8] J. B. Ketterson, *The Physics of Solids*. Oxford University Press, Oxford, 2016.
- [9] L. Pezzè, K. Xhani, C. Daix, N. Grani, B. Donelli, F. Scazza et al., *Stabilizing persistent currents in an atomtronic Josephson junction necklace*, *Nature Communications* **15** (2024) 4831, [2311.05523].
- [10] D. M. Sedrakian and K. M. Shakhbasian, *On a mechanism of magnetic field generation in pulsars*, *Astrofizika* **16** (1980) 727–736.
- [11] M. A. Alpar, S. A. Langer and J. A. Sauls, *Rapid postglitch spin-up of the superfluid core in pulsars.*, *Astrophys. J.* **282** (1984) 533–541.
- [12] V. Allard and N. Chamel,  *$^1S_0$  Pairing Gaps, Chemical Potentials and Entrainment Matrix in Superfluid Neutron-Star Cores for the Brussels–Montreal Functionals*, *Universe* **7** (2021) 470, [2203.08778].
- [13] K. Glampedakis, N. Andersson and L. Samuelsson, *Magnetohydrodynamics of superfluid and superconducting neutron star cores*, *Mon. Not. R. A. S.* **410** (2011) 805–829, [1001.4046].
- [14] M. E. Gusakov and V. A. Dommes, *Relativistic dynamics of superfluid-superconducting mixtures in the presence of topological defects and an electromagnetic field with application to neutron stars*, *Phys. Rev. D* **94** (2016) 083006, [1607.01629].
- [15] P. B. Rau and I. Wasserman, *Relativistic finite temperature multifluid hydrodynamics in a neutron star from a variational principle*, *Phys. Rev. D* **102** (2020) 063011, [2004.07468].
- [16] A. Sedrakian and J. M. Cordes, *Vortex-interface interactions and generation of glitches in pulsars*, *Mon. Not. R. A. S.* **307** (1999) 365–375, [astro-ph/9806042].
- [17] G. Marmorini, S. Yasui and M. Nitta, *Pulsar glitches from quantum vortex networks*, *Sci. Rep.* **14** (2024) 7857, [2010.09032].
- [18] E. Poli, T. Bland, S. J. M. White, M. J. Mark, F. Ferlaino, S. Trabucchi et al., *Glitches in Rotating Supersolids*, *Phys. Rev. Lett.* **131** (2023) 223401, [2306.09698].
- [19] P. Muzikar, J. A. Sauls and J. W. Serene,  *$^3P_2$  pairing in neutron-star matter: Magnetic field effects and vortices*, *Phys. Rev. D* **21** (1980) 1494–1502.
- [20] K. Masuda and M. Nitta, *Magnetic properties of quantized vortices in neutron  $^3P_2$  superfluids in neutron stars*, *Phys. Rev. C* **93** (2016) 035804, [1512.01946].
- [21] Y. Masaki, T. Mizushima and M. Nitta, *Microscopic description of axisymmetric vortices in  $^3P_2$  superfluids*, *Physical Review Research* **2** (2020) 013193, [1908.06215].
- [22] S. Yasui, D. Inotani and M. Nitta, *Coexistence phase of  $^1S_0$  and  $^3P_2$  superfluids in neutron stars*, *Phys. Rev. C* **101** (2020) 055806, [2002.05429].
- [23] Y. Masaki, T. Mizushima and M. Nitta, *Non-Abelian half-quantum vortices in  $^3P_2$  topological superfluids*, *Phys. Rev. B* **105** (2022) L220503, [2107.02448].
- [24] M. Kobayashi and M. Nitta, *Core structures of vortices*

- in Ginzburg-Landau theory for neutron  $^3P_2$  superfluids, *Phys. Rev. C* **105** (2022) 035807, [2203.09300].
- [25] M. Kobayashi and M. Nitta, Proximity effects of vortices in neutron  $^3P_2$  superfluids in neutron stars: Vortex core transitions and covalent bonding of vortex molecules, *Phys. Rev. C* **107** (2023) 045801, [2209.07205].
- [26] A. D. Sedrakian and D. M. Sedrakian, Superfluid Core Rotation in Pulsars. I. Vortex Cluster Dynamics, *Astrophys. J.* **447** (1995) 305.
- [27] A. Sedrakian and J. M. Cordes, Spin Evolution of Pulsars with Weakly Coupled Superfluid Interiors, *Astrophys. J.* **502** (1998) 378–381, [astro-ph/9802102].
- [28] V. Galitski, G. Juzeliūnas and I. B. Spielman, Artificial gauge fields with ultracold atoms, *Physics Today* **72** (2019) 38–44, [1901.03705].
- [29] M. G. Alford and G. Good, Flux tubes and the type-I/type-II transition in a superconductor coupled to a superfluid, *Phys. Rev. B* **78** (2008) 024510.
- [30] T. S. Wood and V. Graber, Superconducting Phases in Neutron Star Cores, *Universe* **8** (2022) 228.
- [31] M. Tinkham, *Introduction to Superconductivity*. McGraw-Hill, New York, 1996.
- [32] M. Borumand, R. Joynt and W. Kluźniak, Superfluid densities in neutron-star matter, *Phys. Rev. C* **54** (1996) 2745–2750.
- [33] N. Chamel and P. Haensel, Entrainment parameters in a cold superfluid neutron star core, *Phys. Rev. C* **73** (2006) 045802.